ELSEVIER

Journal of Nuclear Materials 304 (2002) 182–188

journal of nuclear materials

www.elsevier.com/locate/jnucmat

Aqueous corrosion of aluminum-based nuclear fuel

M.D. Kaminski *, M.M. Goldberg

Argonne National Laboratory, Chemical Technology Division, 9700 South Cass Avenue, Argonne, IL 60439, USA

Received 25 February 2002; accepted 3 May 2002

Abstract

Some aluminum-based nuclear fuels may eventually be disposed in a federally approved repository. As part of the qualification process, experiments are being conducted on uranium-aluminide (UAl_x) fuels to describe corrosion under conditions that could arise during permanent storage. Under the action of intermittent drips of well water at 90 °C, a thin silica-substituted hydrous aluminum oxide gel layer forms over the fuel surface. The exposed fuel oxidizes to produce hydrated aluminum and uranyl oxyhydroxide compounds. In accordance with theory and previous observations with UO_2 fuels, the sequence of alteration products progressed from uranium oxides to uranyl oxyhydroxides such as dehydrated schoepite and becquerelite phases although at a rate that was much faster than for UO_2 fuels. The release or leaching of uranium from the fuel was 0.97 mg U/m^2/d at a pH of 8.4 ± 0.8.

1. Introduction

Department of Energy (DOE)-owned spent nuclear fuel is slated for disposal within the proposed mined geological repository near Yucca Mountain, NV. To enable licensing and acceptance of these fuels at the repository, federal law requires that accurate data and models be generated to allow prediction of the behavior of these fuels in a repository environment. Tests are being conducted to provide information that can be useful in predicting the release of radionuclides while in permanent storage. This paper presents a description of the corrosion of uranium-aluminide (UAl_x) fuel when exposed to small amounts of water that may trickle through a spent fuel container.

These tests elucidate the chemistry of a modified groundwater solution after contact with the spent fuel, dissolution rate of the uranium–aluminum fuel under test-specific conditions, and type and sequence of alteration products. The characterization of colloids will only be addressed briefly but will be the subject of a separate paper.

2. Experimental

Modified groundwater was dripped periodically on pieces of UAl_x fuel. The modified water was prepared by reacting water from the J-13 well near Yucca Mountain at 90 °C for 21 days with crushed core samples of Topopah Spring tuff, the volcanic subsurface material at Yucca Mountain. The modified water is called EJ-13 and is characterized by higher silicon and sodium content than J-13 water (see Table 1) and a pH of 8–8.5.

Representing the great majority of U–Al fuels, the UAl_x fuel was chosen for testing. The UAl_x is a mixture of UAl_2, UAl_3 (primarily), and UAl_4. The fuel specimen was cut from a low-enriched (19% ^{235}U) flat plate. The fuel meat was composed of UAl_x (70.2 wt% U) in aluminum with AG3NE alloy cladding (3% Mg, 97% Al). Square coupons were cut from the middle of the fuel plate and one side of the fuel cladding face was polished to 600 grit to reveal the fuel meat. The resulting monolith was approximately $5 \times 5 \times 2.5$ mm. Fig. 1

---

[*] Corresponding author. Tel.: +1-630 252 4777; fax: +1-630 252 4771/5246.

E-mail address: kaminski@cmt.anl.gov (M.D. Kaminski).

0022-3115/02/$ - see front matter © 2002 Published by Elsevier Science B.V.
PII: S0022-3115(02)00881-4

Table 1
Major elemental composition of EJ-13 water

Element	Concentration (ng/g)
Na	5.54×10^4
K	1.2×10^4
Si	4.1×10^4
Ca	1.1×10^4
Mg	290
Al	560
Fe	250
Zr	1
Au	<0.2
U	0.8
CO_3^{2-}	26×10^6
Cl	15×10^6
F	3.8×10^6
NO_3^-	14×10^6

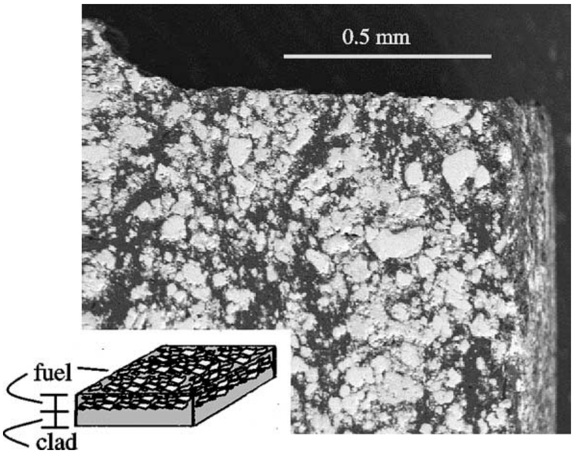

Fig. 1. Electron micrographs of the fuel specimen. The UAl_x grains are indicated by the white, nearly continuous network. The gray regions are aluminum metal (backscatter electron scanning mode, accelerating voltage 20 kV). The inset shows the clad and fuel regions of the specimen. Water was dripped onto the fuel face (top, as shown).

provides a drawing of the fuel specimen showing the orientation of the fuel to the dripping water and an electron micrograph of a corner of the fuel face. Hofman and Snelgrove [1] provide a thorough description of the U–Al fuels.

Fig. 2 contains a description of the experimental configuration, herein referred to as the ‘drip test’ configuration. Five ml of EJ-13 was injected into the base of a stainless steel vessel (60 cm^3 vol.) to maintain saturated humidity and serve as a reservoir for sample collection. The fuel was placed on a Zircaloy or gold screen suspended above the reservoir in a Zircaloy holder. The vessel was sealed, placed in a 90 °C oven and 0.70–0.75 ml EJ-13 water was dripped twice weekly onto the piece of fuel using an external injection port. Three fuel samples were prepared in this manner in separate test vessels. The drops of water flowed over the fuel, through the screen, and were collected in the vessel base. Liquid from the base was completely removed for sample analysis periodically. Test 1 was sampled after 31, 67, 115, 151, and 183 days. Test 2 was sampled after 16 days and Test 3 (using Test 2 fuel coupon after polishing to a clean surface) after 55 days. A control blank (no fuel) was run concurrently to monitor contamination.

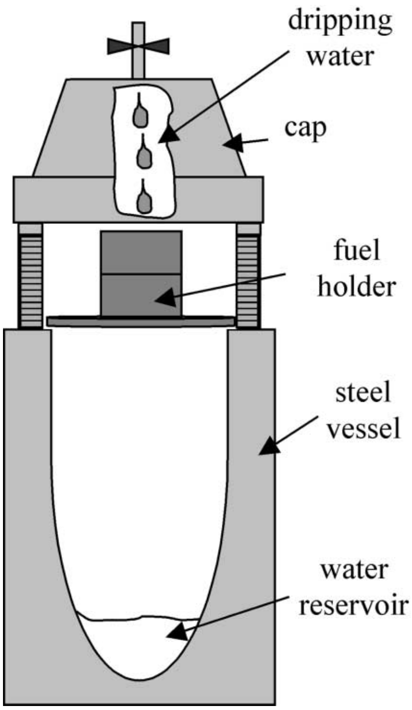

Fig. 2. Cutaway view of the ‘drip test’ configuration.

Prior to sample removal, the test vessels were brought to room temperature by placing in a beaker filled with crushed dry ice for approximately five minutes and then opened. The fuel was removed and set aside for microscopic examination. The entire leachate was removed and acidified with a drop of ultrapure nitric acid prior to elemental determination. Solutions were analyzed at room temperature.

An ‘acid strip’ of the vessel and spent fuel holders was performed (1% HNO_3 at 90 °C overnight) to remove the sorbed fraction including ionic species, precipitates and colloids. Following acid treatment, the vessels and fuel holders were rinsed thoroughly in deionized water and the vessel was reused with the same fuel.

Solution elemental composition was determined by inductively coupled plasma-mass spectrometry using a

Fisons Plasma Quad PQ2, as described elsewhere [2]. Solid samples were characterized by a Hitachi S3000N scanning electron microscope, operated at 5–20 kV in secondary and backscatter electron mode and coupled to a NORAN energy dispersive X-ray spectroscope (EDS). Samples of the fuel surface were removed by razor and characterized using a JEOL transmission electron microscope operating at 200 kV. Some areas of the scrapings were thin enough to perform electron energy loss spectroscopy and electron diffraction.

Release rate values are computed based on the sum of the uranium concentrations in the vessel leachate and acid strips collected during each test interval. They were normalized to the original fuel meat geometric surface area and not to the total fuel monolith surface area, because the latter includes the cladding surface (see Fig. 1). Release rates are expressed in terms of mass of uranium released per original fuel meat surface area per day for the test interval.

3. Previous work

Enough theoretical and experimental information exists in the literature to predict and facilitate interpretation of the paragenesis of the fuel. Most of the data is in conference proceedings or in DOE reports [3] and describes the formation of aluminum hydroxide layers that can be dissolved or eroded. In-reactor tests [4] have shown that the aluminum cladding forms an alteration layer of hydrated aluminum oxides with variable passivity. Defects in the cladding that exposed the fuel produced corrosion of the fuel at rates comparable to similarly run UO_2 fuel tests [4].

Thermodynamically, both the aluminum and uranium within the UAl_x grains favor oxidation [5] as the Gibbs free energy for oxidation for Al and U are both high. The reactions are written as [5]

$$UAl_x + O_2 \rightarrow UO_2 + x\mathrm{Al} \tag{1}$$

in dry air where the free Al can oxidize and,

$$UAl_x + \left(\frac{3}{2}x + 2 + n\right)H_2O \rightarrow UO_2 + \left(\frac{3}{2}x + 2\right)H_2 + \left(\frac{x}{2}Al_2O_3\right)\cdot nH_2O \tag{2}$$

when water is present.

Oxidation of the UO_2 to a higher state is expected to be quite rapid since no crystallographic rearrangement is necessary [6]. In fact, Openshaw and Sheir [5] could not find the UO_2 layer predicted by Eq. (2) and the solution chemistry – oxidizing, prevalent hydroxide species – favors oxidation to and dissolution of uranyl species [6] where

$$UO_2 \rightarrow UO_2^{2+} + 2e^-. \tag{3}$$

From UO_2 fuels tests [7,8] one would expect oxyhydroxide precipitates to form such as dehydrated schoepite $(UO_2)O_{0.25-x}(OH)_{1.5+2x}$ $(0 \leqslant x \leqslant 0.15)$ and becquerelite $Ca(UO_2)_6O_4(OH)_6(H_2O)_8$, with the uranyl silicates like soddyite $(UO_2)_2SiO_4(H_2O)_2$ forming from the early-formed uranyl oxyhydroxides [6]. This information provides some theoretical justification for comparing the corrosion of UAl_x fuel to the UO_2 fuels but, as shall be shown, there are significant fundamental differences in the paragenesis of UAl_x compared to UO_2.

4. Results and discussion

Once exposed to drip test conditions, the fuel surface tarnished to a dark-gray speckled in white. Only after 183 days were rust-colored and yellow precipitates visible on isolated spots of the fuel surface. Mechanically, the fuel coupon remained intact, stiff, and not friable.

4.1. Hydrated Al–Si alteration layer

The fuel surface oxidized quickly to form a variably thick hydrated aluminum oxide layer. This layer may be more appropriately termed a hydrogel since it is excessively hydrated under the saturated water conditions. Its thickness varied with time (<100 nm to 5 μm) and position on the fuel face [1] and cracks formed as the surface dried when removed for analysis (gel syneresis). The hydrogel layer was not observed to be greater than 5 μm in thickness (see Fig. 3) and was readily observed on 60–100% of the surface for a particular analysis period, with the remainder of the fuel surface exposed to the humid atmosphere directly or through a vanishingly thin alteration layer (i.e., less than the ~100 nm method detection limit). The smooth surface of the gel is shown in Fig. 4. X-ray analysis showed silicon to be ubiquitous about the gel. This may be a result of precipitated silica (SiO_2) or from incorporation of silica into the hydrogel structure as described by Plank [9], or both. The formation of aluminosilicate hydrogels from hydrated aluminum oxide gels seems a likely outcome and can be described by

$$Al(OH)_3 \cdot nH_2O + SiO_4^- \rightarrow Al(OH)_2SiO_4 \cdot nH_2O + OH^-, \tag{4}$$

---

[1] Samples were stored in air prior to examination. The hydrogel layer thickness that was measured will be smaller than the actual gel thickness during test conditions due to shrinkage from water loss (syneresis) [9].

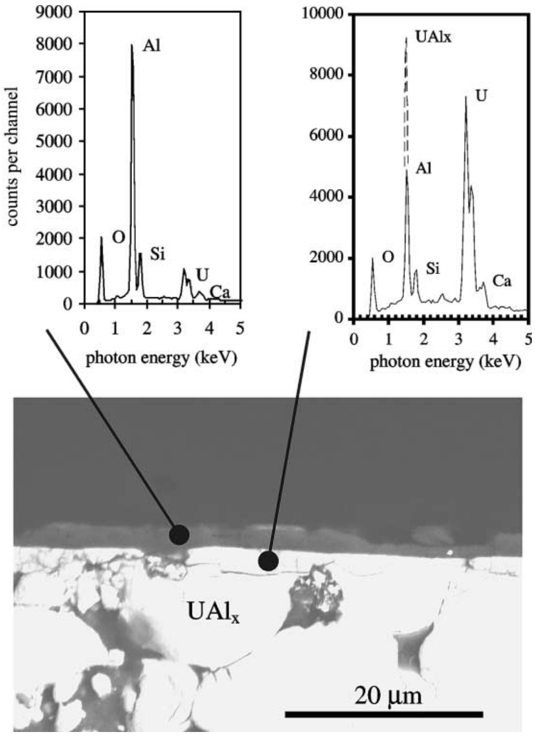

Fig. 3. Transverse image of the reacted fuel after 183 days and EDS of hydrogel (left) and uranium alteration layer (right). The relative Al peak (dashed curve labeled ‘UAl$_x$’) for unaltered UAl$_x$ is provided for comparison. Note the presence of Ca and Si in these alteration layers (accelerating voltage 20 kV, magnification shown on micrographs).

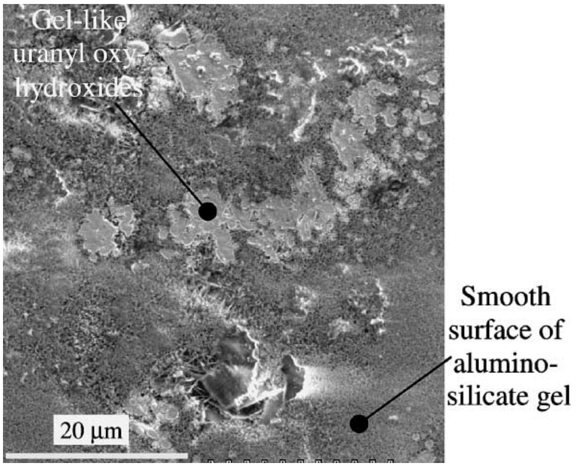

Fig. 4. Electron micrograph of UAl$_x$ fuel surface showing aluminosilicate hydrogel morphology. (Magnification and scale bar shown in micrograph, accelerating voltage 5 kV in secondary electron mode.)

where $Al_2O_3 \cdot 3H_2O$ is identical to $2Al(OH)_3$ [9]. Inclusion of silica into the gel would thus require the release of hydroxyl anions and concomitant rise in pH. In slightly alkaline pH, the time required to form a gel from dissolved Al ions (gelation or syneresis) is probably near its minimum and could be less than a few hours at pH 8–9 [9]. This is significant because it reveals that the hydrogel has time to stabilize between incoming groundwater injections and may not form as readily under a flowing or bathtub system. In addition, since this gel is aluminum based, no such gel would form during the corrosion of UO_2 fuels.

The gel can be disaggregated (or peptized), releasing individual colloids that may play an important role in radionuclide disposition and transport. Silica alumina gels can have base-exchange capacities explained by the substitution of Al in terminal positions in the structure [9] and the composition of the gel will reflect the relative concentration of the silicate and aluminate in the solution from which it was formed [10]. In the UAl$_x$ fuel, EDS revealed that the hydrogel is dominated by Al, but some areas have comparable Si concentration, which suggest that the local dissolved Si concentration in the hydrogel varied with position on the fuel surface. By remaining in intimate contact with actinides and fission products released from the corroding UAl$_x$ grains and dissolved in the gel, the gel can retard the release of these radioisotopes or act as a potentially stable transport vehicle once released by peptization. A similar retardation effect is reported during the alteration of nuclear waste glasses [11]. The properties of colloids found in this test configuration will be described in a separate publication.

4.2. UAl$_x$ oxidation

Exposed UAl$_x$ fuel grains underwent oxidation during the test period of 183 days to a variety of products. As is described in detail below, the sequence of reactions was initiated by formation of a superficial hydrogel within which limited grain dissolution and ion diffusion occurred. Diffusion of ionic species in a hydrogel can be similar to that in water [12]. In situ mineral formation occurred within the gel and resulted in a series of uranyl oxides, oxyhydroxides, and silicates that have been observed previously in UO_2 fuel oxidation tests under similar dripping water conditions. However, the UAl$_x$ oxidation reactions occurred at a much faster rate than those of the UO_2 fuel, and it is suggested that retention of the dissolved and precipitated species within the oxic hydrogel provided reactant concentrations and conditions appropriate for accelerated oxidation.

Within 16 days of test start (the first time the tests were opened for examination), the hydrogel layer formed. Where UAl$_x$ grains had been exposed on the surface, clusters of uranium-rich precipitates were observed. Fig. 5(a) shows a representative cluster of spherical precipitates of uranyl oxyhydroxides on top of UAl$_x$ grains observed at 16 days. When the sample dried

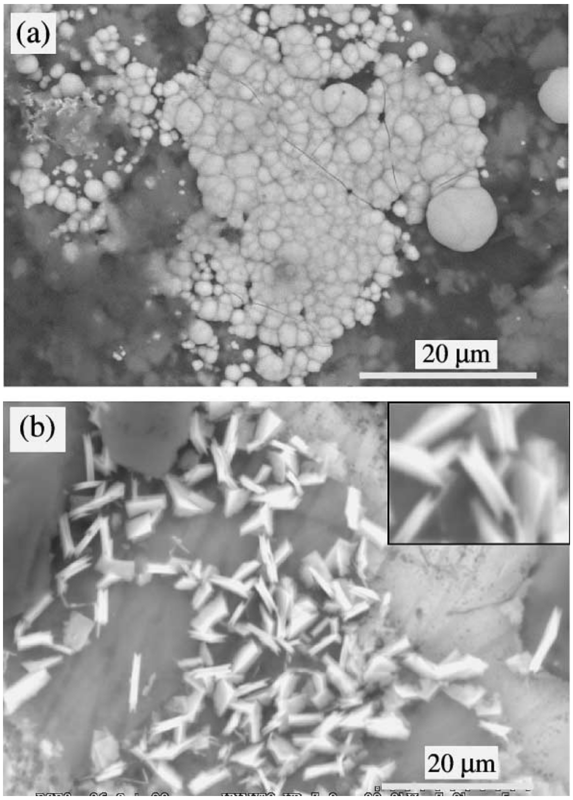

Fig. 5. (a) Uranyl oxyhydroxides atop the corroded UAl_x grains after 16 days on fuel from Test 2. Upon drying platelets crystallize. (b) Note the platelet splitting, magnified in the inset, a phenomena consistent with dehydration of the oxyhydroxides of uranium. (Magnification and scale bar shown in micrographs. Accelerating voltage 20 kV.)

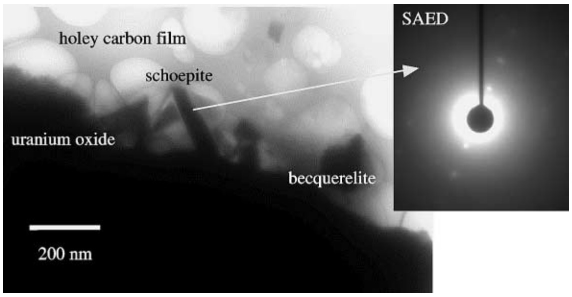

Fig. 6. Image showing alteration phases on the surface of uranium oxide. Based on electron diffraction and EDS analysis, disordered uranyl crystal phases were identified as dehydrated schoepite and becquerelite.

for several days at room temperature, the spherical precipitates evolved into small platelets, 1–2 μm on edge, that showed splitting patterns consistent with the uranyl oxyhydroxide, dehydrated schoepite (Fig. 5(b)). The uranyl oxyhydroxides are well known [6] to form as early corrosion products of uraninite (UO_2) and the presence of dehydrated schoepite was confirmed by transmission electron microscopy and electron diffraction (see Fig. 6).

At each fuel sampling, uranyl oxyhydroxides were observed on the fuel surface. Fig. 3 shows EDS spectra of the hydrogel region (<2 μm thick) and the altered fuel layer immediately beneath it after 183 days in test. Both spectra indicate the presence of U, Al, Ca, Si, and O, but the altered layer shows significant depletion of Al relative to that present in UAl_x, while the hydrogel spectrum indicates an abundance of aluminum oxides. The presence of dissolved Ca and Si can lead to the formation of the calcium uranyl oxyhydroxide, becquerelite (observed in Fig. 6), and presumably to uranyl silicates such as uranophane. Although uranyl silicates were not identified in this study, it is speculated that their formation was kinetically limited [6].

The uranyl oxyhydroxides were observed in several morphologies. Fig. 5 illustrates spherical and plate-like structures, and Fig. 7 illustrates worm-like textures and triply-terminated elongated structures. The worm-like morphology in Fig. 7(a) is consistent with the dehydrated schoepite structure described by Taylor et al. [13]. The structures shown in Fig. 7(b) were observed in the 115- and 183-day samplings when the hydrogel had dissolved sufficiently. Highly fractured/altered UAl_x grains gave rise to thin, elongated structures with triple terminations. Other elongated crystals with flat terminations were observed within and above the hydrogel (not shown).

The release rate for uranium is shown in Fig. 8. A total of a 7.9 μg of uranium (<0.02% of total inventory) [2] was released after 183 days from fuel from Test 1 for a normalized rate of 0.8 mg U/m^2/d (range 0.2–1.3 mg/m^2/d for four measurements) and an average of 0.97 mg U/m^2/d (range for three tests 0.2–2.9 mg U/m^2/d) for all three tests. Assuming the uranium was released in the dissolved state (UO_2^{2+}) and the oxides reached equilibrium with the fluid, the average uranium concentration carried by the dripping water was 2×10^{-7} to 2×10^{-6} molar. This value is consistent with control of uranium solubility by schoepite at pH 8 [14]. The present release rates can be adjusted to reflect normalization to the surface area of UAl_x grain by dividing by 0.7 for an average rate of 1.4 mg U/m^2/d. This value is comparable to drip tests on irradiated commercial UO_2 fuels (0.7–1.5 mg/m^2/d) [15,16] at 90 °C, a result that appears logical since UAl_x grains will form UO_2 intermediates toward eventual formation of the uranyl species. However, this

---

[2] Assuming the fuel specimen contains 70% UAl_x, and the fuel meat is 49 wt% U.

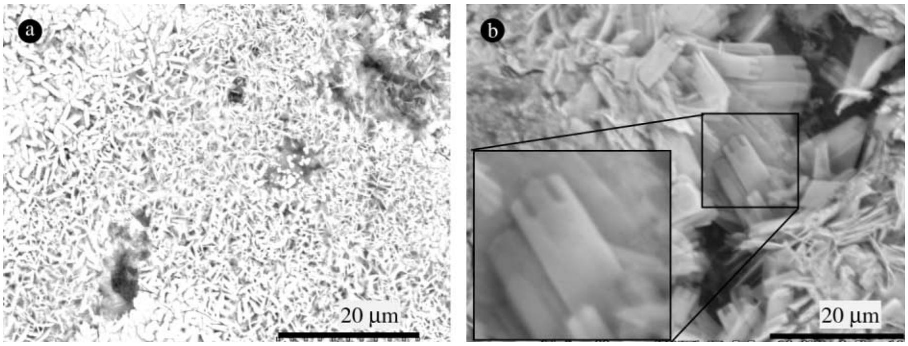

Fig. 7. Micrographs of hydrogel layer. (a) Worm-like patches were observed. These are similar in morphology to dehydrated schoepite found in polished UO_2 samples oxidized in humid air [13]. (b) Elongated uranium-rich crystals with triple terminations were found after 183 days of testing.

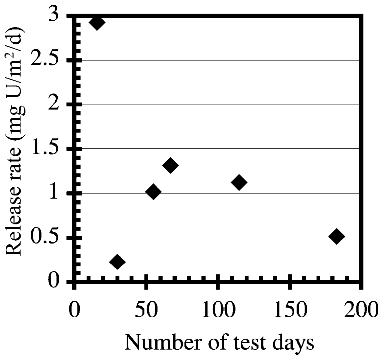

Fig. 8. Uranium release rates for Test 1 (day 31, 67, 115, and 183), Test 2 (day 16) and Test 3 (day 55).

conclusion simplifies the actual reaction mechanism that must account for the hydrogel layer chemistry and increased reaction rates describing the formation of the uranyl oxyhydroxides.

5. Conclusions

The drip test conditions are conducive to the synthesis of a thin silica-substituted aluminum hydrogel. Uranyl oxyhydroxides form concurrently and crystallize as platelet masses consistent with the uranyl oxyhydroxides. Electron diffraction confirmed the presence of poorly formed dehydrated schoepite and becquerelite phases and agrees with phases determined in the initial years of drip tests on UO_2 although their presence comes much earlier than in the UO_2 tests. Although the release rates for U were comparable to UO_2 fuel tests, this overly simplifies the data since it has been shown that the hydrogel layer significantly retains uranyl precipitates and provides conditions favorable for accelerated oxidation. Moreover, the release and disposition of actinides like Np, Pu, and Am may be strongly affected by the cationic exchange properties of the hydrogel or colloids generated by the gel. This can greatly influence accurate modeling of radioisotope transport. Similar tests on irradiated fuels, as described here, will shed light on the role that the hydrogel might play in actinide release.

Since the initiation of this program, a decision has been made to condition the aluminum-based fuels in a ‘melt-dilute’ process [17]. This process requires melting the current fuel and adding depleted uranium, aluminum, and neutron absorbers to create an alloy with low uranium enrichment and reduced spent fuel volume. It also reduces criticality risk and creates a material that is less amenable for use in weapons. The effect of the melt-dilute process on corrosion rate, mineral products, and isotope releases will have to be evaluated since the process redistributes the fission and activation products (during the melt) as well as the major elements in the fuel. If the data suggest that the actinides are retained in the UAl_x grains, the release rates may be appropriately compared between the UAl_x and the melt-dilute formulation.

Acknowledgements

The authors extend a special thanks to the members of the Spent Nuclear Fuel Group in CMT and R. Finch for useful discussion. The authors acknowledge the fine craftsmanship of W. Brown and the members of the CMT machine shop. The leachate analysis performed by S. Wolf, Y. Tsai, and K. Quigley was much appreciated, as was the TEM analysis by J. Holly and E. Buck. Also, thanks to the members of the AGHCF at Argonne for sample preparation and useful documents and information. This work was supported by the National Spent Nuclear Fuel Program Release Rate Program and the US Department of Energy, under contract W-31-109-ENG-38.

References

[1] G. Hofman, J. Snelgrove, Mater. Sci. Technol. 10A (1994) 45.

[2] S.F. Wolf, J. Radioanal. Nucl. Chem. 235 (1–2) (1998) 207.

[3] L.B. Lundberg, M.L. Croson, Corrosion of spent advanced test reactor fuel, Conf-941297-9, 1994.

[4] K. Vinjamuri, R.R. Hobbins, Nucl. Technol. 62 (1983) 145.

[5] P.R. Openshaw, L.L. Sheir, Corros. Sci. 4 (1964) 335.

[6] R. Finch, T. Murakami, Rev. Mineral. 38 (1999) 91.

[7] D.J. Wronkiewicz, J.K. Bates, S.F. Wolf, E.C. Buck, J. Nucl. Mater. 238 (1996) 78.

[8] R.J. Finch, E.C. Buck, P.A. Finn, J.K. Bates, Mater. Res. Soc. Symp. Proc. 556 (1999) 431.

[9] C.J. Plank, J. Colloid Sci. (1947) 413.

[10] I. Krznaric, T. Antonic, B. Subotic, Zeolites 19 (1997) 29.

[11] S. Gin, I. Ribet, M. Couillard, J. Nucl. Mater. 298 (2001) 1.

[12] H.K. Henisch, Crystal Growth in Gels, Pennsylvania State University, University Park, PA, 1970.

[13] P. Taylor, D.D. Wood, D.G. Owen, J. Nucl. Mater. 223 (1995) 316.

[14] Y. Chen, T. Wolery, R. Gaylord, W. Halsey, Summary of dissolved concentration limits, analysis model report, AMR-WIS-MD-000010 Rev.00, Office of Civilian Radioactive Waste Management, April 2001.

[15] P.A. Finn, R. Finch, E. Buck, J. Bates, Mater. Res. Soc. Symp. Proc. 506 (1998) 123.

[16] P.A. Finn, E.C. Buck, J.C. Hoh, J.K. Bates, Spent fuel's behavior under dynamic drip tests, in: Global '95, International Conference on Evaluation of Emerging Nuclear Fuel Cycle Systems, Versailles, France, September 1995.

[17] T.M. Adams, H.B. Peacock, F.C. Rhode, N.C. Iyer, Mater. Res. Soc. Symp. Proc. 556 (1999) 495.